Improvement of interlukin-18 aggregation and activity by replacement of surface cysteine by serine

Jirakrit Saetang[1], Niran Roongsawang[2], Surasak Sangkhathat[1], Supayang Voravuthikunchai[1], Natnaree Sangkaew[1], Napat Prompat[1], Teerapol Srichana[1], and Varomyalin Tipmanee[1]

[1]Prince of Songkla University
[2]National Science and Technology Development Agency

April 16, 2024

Abstract

Interleukin-18 has been proposed for cancer immunotherapy for a long time. However, the presence of IL-18 binding protein (IL-18BP) and the unstable form of IL-18 caused the low impact of this protein in human clinical trials. To overcome this, we performed the mutagenesis targeting surface cysteines (C38, C68, C76, and C127) on our modified IL-18 to prevent intermolecular disulfide bond formation. The ORF of wild-type, IL-18 DM and IL-18 DM1234 were synthesized and expressed in E. coli. All IL-18 were refolded by step-wise dialysis and tested for protein aggregation by ProteoStat protein aggregation assay. All recombinant IL-18 were also investigated for activity by IFN-γ induction assay. The structure of modified IL-18 was visualized by molecular dynamic (MD) simulation. The results showed that IL-18 DM1234 demonstrated the lowest aggregation signal compared to others. This protein also displayed higher activity than wild-type and IL-18 DM about 10 and 2.8 times, respectively. MD simulation revealed the binding site I of IL-18 DM1234 was the part mostly affected by C-to-S substitution. In conclusion, this is the first report for IL-18 that the modifications by mutagenesis improved both activity and stability and this IL-18 may be used for medical purposes in the future.

1. Introduction

Interleukin-18, IL-18, is a cytokine that plays a role in many aspects of human immunological system. This cytokine was previously named as interferon-γ-inducing factor that reflected its function in human physiology (Okamura et al., 1995). Nowadays, this cytokine has been recognized as one of the cytokine that promote type 1 helper T cell response which is essential for anti-tumor immunity (Fabbi et al., 2015; Nakamura et al., 2018). Moreover, IL-18 also polarizes human NK cells to develop a distinct helper differentiation phenotype ($CD83^+CCR7^+CD25^+$) and stimulate cytotoxic lymphocytes to enhance IFN-γ secretion, granule-mediated cytotoxicity and Fas ligand expression (Mailliard et al., 2005; Srivastava et al., 2010). From these reasons, the using of IL-18 in cytokine therapy for cancer has been established and developed in both animal and human studies (Robertson et al., 2006, 2008). However, although cancer patients were good tolerated to this cytokine, the efficacy was still limited due to its high-affinity antagonist IL-18-binding protein (IL-18BP) which is increased in many cancers (Srivastava et al., 2010). Moreover, the precipitation or aggregation which is commonly found in recombinant cytokine therapeutics is another problem that may cause the loss of activity and increase the risk of immunogenicity (Lipiäinen et al., 2015).

To overcome this immunological inhibition of IL-18BP, many studies tried to apply the knowledge of molecular engineering to this protein by site directed mutagenesis and protein engineering. A study showed that the substitution of amino acid of IL-18 from glutamic acid to alanine at position 6 (E6A) and lysine to alanine at position 53 (K53A) could enhance the activity of IL-18 and reduce the affinity to IL-18BP

(S. H. Kim et al., 2001). In addition, they also changed the type of mutation of E6 from E6A to E6K and found that this mutation increased the activity of IL-18 to induce IFN-γ about 3-8 times compared to wild-type (S.-H. Kim et al., 2002). Another research highlighted the change of intramolecular core threonine at position 63 to alanine enhanced the activity of IL-18 approximately 3 times compared to native IL-18 (Swencki-Underwood et al., 2006). Recently, decoy-resistant IL-18 has been developed for applying to cancer immunotherapy. This modified IL-18 was reported to be less sensitive to IL-18BP than native IL-18 and promoted the polarization and stimulation of effector cytotoxic T cells and natural killer cells, respectively (T. Zhou et al., 2020). While most of studies focused on IL-18 activity improvement, some works tried to develop the low aggregating IL-18. For example, the surface cysteine of IL-18 was found to be associated with protein aggregation and instability and this led to the replacement by serine at position 38, 68, 76 and 127, which caused IL-18 to be tolerated to oxidative stress and decreased the aggregation (Yamamoto et al., 2004).

In previous work, we have developed the modified IL-18 with the high activity about 16 times more than wild-type protein (Saetang et al., 2016). This engineered IL-18 was found to be a potent inducer for IFN-γ induction from NK-92MI cell. Moreover, it showed the anti-tumor activity that promoted type 1 helper T cell and cytotoxic T lymphocyte in CT26-WT colon cancer animal model (Saetang et al., 2020). However, according to the stability testing from the other works, IL-18 tend to form multimer which led to the inactive IL-18 aggregates (Kato et al., 2003; Li et al., 2003; Yamamoto et al., 2004). This problem was also found in our work when the high concentration of modified IL-18 was prepared. Therefore, to improve the quality of modified form of IL-18 to be more stable and less aggregated, we tried to rely on the method that changed the surface cysteine by serine to our IL-18.

This study described the generation of double modified IL-18 with the increasing of both activity and stability. Interestingly, the replacement of cysteine by serine also improved the activity of engineered IL-18 indicating the less aggregation led to the higher activity.

2. Materials and methods

2.1 Plasmid construction and protein expression

All plasmids were synthesized and obtained from GenScript company (NJ, USA). Open reading frame (ORF) of IL-18 with optimized codon for*E. coli* expression system was inserted between *Nde* l and*Eco* RI restriction sites of pET28a expression vector. The mutant IL-18 including IL-18 E6K+T63A double mutation (IL-18 DM) and IL-18 E6K+T63A+C38S+C68S+C76S+C127S (IL-18 DM1234) were also obtained from the same source with similar restriction sites and vector. All recombinant plasmids (pET28a-IL-18WT, pET28a-IL-18DM and pET28a-IL-18DM1234) were transformed to *E. coli* Rosetta2 (DE3) pLysS and selected by Luria Bertani (LB) agar (Sigma-Aldrich, USA) containing 34 mg/ml of chloramphenicol (Invitrogen, USA) and 50 mg/ml of kanamycin (Invitrogen, USA). The selected clones were then used for IL-18 production. Briefly, each type of IL-18 bearing*E. coli* was grown in LB broth containing 34 mg/ml of chloramphenicol and 50 mg/ml of kanamycin and incubated in shaker incubator (Wiggens, Germany) at 37 °C, 200 rpm till OD600 reach 0.6. After that, 1 M IPTG (Sigma-Aldrich, USA) was then added to the culture with the final concentration of 0.1 M and incubated at 25 °C in shaker incubator with 200 rpm for 5 h. Bacterial cells were then harvested by centrifugation at 10,000 rpm for 10 min, resuspended in 10 ml PBS and sonicated on ice with 60% amplitude and pulses of 10s: 15s for 5 min. Cell lysate was then centrifuged for 10 mins at 10,000 rpm at 4 °C. The supernatant and cell pellet were separated and checked by 12% gel SDS-PAGE.

2.2 Stepwise refolding

The pellet from sonication step was washed by 25 ml PBS 3 time and centrifuged at 10,000 rpm for 10 min. Pellet was then collected, weighted and resuspended in solubilization buffer [base buffer (50 mM Tris-HCl, 150 mM NaCl, 100 mM Glycine, 20% Glycerol, pH 8.0) containing 8 M urea] with the final concentration of 2-8 mg/ml. The suspension was then mixed in orbital shaker for 30 min and centrifuged at 15,000 rpm for 15 min before filtrating with 0.45 μm syringe filter. The supernatant was then dialyzed with slide-A-Lyzer G2 dialysis cassettes (Thermo Scientific, USA) toward 1 L of base buffer containing 6M urea for 4 h at 4°C.

During this step, 500 mL of base buffer was added to dialysis buffer every 6 or 12 h for 4 times. Finally, the dialysis cassette with solubilized inclusion body was placed in 2 mL purely base buffer for 6 h. The refolded IL-18 were then harvested and kept at 4 °C until use.

2.3 Western blotting

After performing 12% SDS-polyacrylamide gel electrophoresis, protein was then transferred onto a polyvinylidene difluoride (PVDF) membrane (Bio-Rad, USA) with electroblotting at 35 volts for 16 hours in transfer buffer. Non-specific protein was blocked by incubating the PVDF membrane with TBST containing 3% (w/v) BSA (Sigma-Aldrich, USA) for 1 hour, followed by washing with TBST three times. Membrane was then stained with specific mouse anti-human IL-18 (R&D systems, USA) at 1:3,000 dilution for 1 hour and washed three times for 5 min each in TBST with gentle agitation. Horse radish peroxidase-conjugated goat anti-mouse IgG (R&D system, USA) was added at a dilution of 1:10,000 in TBST containing 3% (w/v) BSA and incubated for 1 hour at room temperature. After washing for three times in TBST, IL-18 were detected by Luminata Forte Western HRP substrate (Millipore, USA) with UVITEC Cambridge Gel Documentation System (UVITEC, UK).

2.4 Liquid Chromatography with tandem mass spectrometry (LC-MS/MS)

LC-MS/MS analysis was performed by commercial service of Proteomics International Company, Australia. Protein samples were trypsin digested and peptides extracted according to standard techniques (Bringans et al., 2008). Peptides were analyzed by electrospray ionization mass spectrometry using the Shimadzu Prominence nano HPLC system (Shimadzu, Japan) coupled to a 5600 TripleTOF mass spectrometer (Sciex, USA). Tryptic peptides were loaded onto an Agilent Zorbax 300SB-C18, 3.5 μm (Agilent Technologies, USA) and separated with a linear gradient of water/acetonitrile/0.1% formic acid (v/v). Spectra were analyzed to identify proteins of interest using Mascot sequence matching software (Matrix Science, UK) with UniProt database.

2.5 Protein aggregation assay

Each type of recombinant refolded IL-18 was subjected to buffer exchange by Vivaspin ultrafiltration unit (Satorius, Germany) toward PBS. To generate IL-18 aggregates, 40 μg/mL of each type of protein was incubated at 37 °C for 16-18 h in shaker incubator at 220 rpm. Protein aggregation assay was performed by using ProteoStat Protein Aggregation Assay (Enzo Lifesciences, USA). Protein was then loaded in triplicate in 96 well fluorescent microplates before adding ProteoStat detection dye. The reaction was incubated for 15 min in the dark at room temperature. The fluorescent signal was then determined at excitation at 485 nm and emission at 620 nm by Varioskan LUX multimode microplate reader (Thermo Scientific, USA)

2.6 Ιντερφερον-γ ινδυστιον ασσαψ

NK-92MI cell were maintained in completed α-MEM medium supplemented with 12.5% FBS and 12.5% horse serum at 37°C in CO_2incubator and was used to evaluate the activity of each type of IL-18. The experiment was performed as previously described. Briefly, cells were suspended in 0.2 ml complete media at 0.5 × 10^6cell/ml. The induction was performed by using each type of recombinant IL-18 at the concentration of 75, 150 and 300 ng/ml with 0.5 ng/ml of human IL-12. After 16–18 h of incubation at 37°C in CO_2incubator, the supernatants were collected and IFN-γ ELISA assay was then performed by using Human IFN-γ Quantikine ELISA Kit (R&D system, USA).

2.7 Molecular dynamic simulation

Human interleukin-18 (IL-18) crystal structure was taken from RCSB Protein Data Bank, an ascension code 3WO2 (Tsutsumi et al., 2014). The co-crystallized solvents were then removed from the structure. The cysteine-serine replacement was performed using FoldX package (Schymkowitz et al., 2005). All ionizable amino acids was set as a default state at pH 7.0. A neutral histidine was set as a singly -protonated histidine (HIE in AMBER name). No doubly protonated histidine and disulfide linkage was observed. The IL18 protein was then solvated using the TIP3P water rectangular box with the distance of 14 Å from protein

surface. The system was neutralized using sodium ion, and sodium chloride (NaCl) was added to create 0.15 mol L-1 NaCl solution (Saetang et al., 2016) using AMBER20 force field (Case et al., 2021) via Leap module in AMBER20 package. In total, the system consisted of monomeric IL18, 4 sodium ions, 33 NaCl pairs, and 11437 TIP3P waters.

The wild-type and mutated IL18 structures were then energy-minimized using steeping descent and conjugate gradient methods for 1000 and 1000 steps, respectively under a periodic boundary condition. The minimized structure was taken into canonical (NVT) simulation at 37°C (310 K) in which all protein positions were restrained by harmonic potential. The temperature was controlled using Langevin thermostat. All nonbonded and electrostatic interactions were calculated using a cutoff of 16 Å. Each NVT restrained simulation was executed for 200 picoseconds (ps) with a time step of 1 femtoseconds, which a force constant of 200, 100, 50, 20 and 10 kcal/mol Å-2 , in total of 1 nanosecond (ns). To apply the pressure of 1.013 bar (1 atm), the system was changed into isobaric-isothermal (NPT) simulation. The temperature and the pressure were regulated using weak-coupling algorithm (Berendsen et al., 1984). The NPT simulation lasted 120 ns with a time step of 2 fs. The first 60 ns simulation was omitted and the last 60 ns simulation was taken into the analyzed trajectory. All energy minimization and molecular dynamics processes were carried out with PMEMD module implemented in AMBER20 package. In addition, the trajectory in AMBER coordinate format (.mdcrd) file was converted into the Protein Data Bank (PDB) file using cpptraj in AMBER20 package. The structure visualization and interaction analysis of all IL18 cases were all performed using VMD package (Humphrey et al., 1996).

2.8 Statistical analysis

The data are presented as means ± SD. The significance of the data was calculated by using Student's t-test. P values less than 0.05 was considered statistically significant.

3. Results

3.1 Structure analysis of surface cysteine of IL-18

Although the analysis of cysteine residues on the surface area of IL-18 was described in the previous work (Yamamoto et al., 2004, p. 18), the source of PDB structure was from NMR analysis (PDB no. 1J0S) (Kato et al., 2003, p. 18). Currently, IL-18 structure was crystalized together with its receptors (Tsutsumi et al., 2014, p. 18) allowing the researchers to study the role of each amino acid residue of human IL-18 on its interaction to the receptor. We decided to re-analyze the role of surface cysteine on its interaction to receptor by using crystalized structure (PDB no. 3WO3). As showed in Fig. 1A and 1B, the surface cysteine including C38, C68, C76 and C127 can be found independently and are not interacted to each other. The direction of thiol side chain of most cysteine showed toward the surface of IL-18 molecule. No intramolecular interaction was found suggesting the role of these surface cysteine for intermolecular interaction. Additionally, when the analysis of these amino acids was considered in binding mode with its receptor, IL-18 receptor α, all of these cysteines were not found to be important for the receptor binding (Fig. 1B). This is in accordance with the analysis from the NMR structure that showed the possibility of amino acid replacement did not disrupt the interaction between IL-18 and IL-18 receptors (Yamamoto et al., 2004). Therefore, we applied the mutation from this work to improve our engineered human IL-18.

3.2 Expression and refolding of recombinant proteins

The expression of each type of IL-18 was performed in *E. coli*Rosetta2 (DE3) pLysS. After cell lysis by using sonication method, both soluble and inclusion body of crude protein were analyzed by SDS-PAGE. Figure 2 demonstrated that a protein band about 20 kDa corresponding to mature form of human IL-18 was detected in both soluble fraction and inclusion body extracted from *E. coli* harboring pET28a containing IL-18 ORF insert while the same molecular weight was not observed in transformant having an empty vector (data not shown). However, more than 80% of this protein was found as inclusion form in all type of IL-18 (Fig. 2A lane 4, 5 and 6). This result suggested that recombinant human IL-18 was successful expressed in *E. coli* mostly as inclusion body. Therefore, in order to refold the protein to correct the structure of

IL-18, step-wised refolding methods were then performed after washing steps. The result showed that the purity of the protein after refolding step was greater than 95% in SDS-PAGE analysis with yield less than the beginning source (Fig. 2B). Western blotting was also used to demonstrate the specific protein bands by anti-human IL-18 antibody (Fig. 2C). We validated the recombinant IL-18 by excising the protein band from the gel and subjecting to LC-MS/MS analysis. Tryptic digestion of this protein provided 9 fragments of peptides covered about 48.0% of pro-form of IL-18 or 58.8% of mature form IL-18 (Fig. 3A and 3B). These data suggested that this refolded IL-18 was mature IL-18.

3.3 IL-18 DM1234 showed the lower aggregation capability with the higher activity

To evaluate the effect of the replacement of surface cysteine to serine on IL-18 aggregation, the oxidative stress of protein was induced by shaking the protein at 220 rpm in shaker incubator. The heat was also used to increase the energy of the reaction. After 16-18 h. of induction, the aggregated protein was then measured by ProteoStat protein aggregation assay. The result demonstrated that no difference in protein aggregation was observed between IL-18 DM and wild-type (Fig. 4A). However, IL-18 DM1234 showed significant decrease in protein aggregation determined by ProteoStat dye (Fig. 4A). This mutation could lower the aggregation ability of IL-18 DM1234 about 1.79 and 1.63 folds compared to IL-18 wild-type and IL-18 DM, respectively. Interestingly, when interferon-γ (IFN-γ) induction assay was performed with all three types of IL-18, the mutations of cysteine to serine showed the statistically increasing capability to stimulate the production of IFN-γ from NK-92MI cells (Fig. 4B). The levels of IFN-γ of IL-18 DM1234 indicated the higher efficacy approximately 10.0 and 2.8 folds compared to wild-type and DM IL-18, respectively. This suggested that the mutation of surface cysteine to serine enhanced the ability of IL-18 to activate NK-92MI in either way.

3.4 Mutation of surface cysteine by serine may improve the stabilization of IL-18 DM1234 to its receptor

According to the result from IFN-γ induction assay, molecular dynamic (MD) simulation was performed to investigate the role of substitution of surface cysteine by serine on structure of IL-18, which may affect the activity of this protein. After 120 nanoseconds of MD simulation with physiological parameters, all structures (WT, DM and DM1234) were visualized and aligned by VMD program to determine the difference in structural conformation of each type of IL-18. The result showed that the obvious conformational change of IL-18 DM1234 was observed at α-helix as a part of binding site I when compared to IL-18 DM (Fig. 5A and 5B). This binding site I contains methionine 33 (M33) and aspartate 35 (D35) identified as the important binding residues of IL-18 to IL-18 receptor α (Kato et al., 2003). Figure 5B demonstrated this alteration led to the higher similarity of this region between IL-18 WT and IL-18 DM1234, which may improve the stabilization of IL-18 DM1234 by IL-18 receptor like the native structure. Importantly, when looked deeper into the direction of amino acids in this area, we found that D35 changed its direction closer to valine 125 (V125) and serine 127 (S127) of IL-18 receptor compared to IL-18 WT (Fig. 5C). Structural alignment revealed that the distance between D35 of IL-18 DM1234 and V125 and S127 of IL-18R were in range of 2.88-4.72 A@ (Fig. 5B) while D35 of IL-18 WT showed the higher distance with 5.28 and 5.95 A@ between V125 and S127, respectively (Fig. 5C). Moreover, D35 of IL-18 DM also showed the higher distance of these molecular pairs (4.35 and 4.95 A@ for V125 and S127, respectively) when compared to IL-18 DM1234 (Fig. 5D). This result suggested that the substitution of surface cysteine by serine may contribute to the alteration of IL-18 DM1234 activity through conformational change at binding site I.

4. Discussion

IL-18 has been proposed as a candidate for cancer treatment for a long time. Many studies have revealed the role of this cytokine as inducing factor for IFN-γ, which plays an important role in anti-cancer immunity (Castro et al., 2018). However, the limitation of using this cytokine was demonstrated by the low impact of this cytokine in clinical trials (Robertson et al., 2006). This may be due to the presence of natural inhibitor, IL-18 binding protein, that increases in several types of cancers (Srivastava et al., 2010). Interestingly, many research tried to improve both efficiency and stability of this protein, mainly by protein engineering.

The popular technique that has been applied to modify this protein is site-directed mutagenesis based on the knowledge of binding mode of IL-18 to its receptor (Kato et al., 2003; S. H. Kim et al., 2001; S.-H. Kim et al., 2002; Saetang et al., 2016; Yamamoto et al., 2004). Most of studies showed the successful development of engineered IL-18 with enhancing activity and bioavailability, especially the development of the decoy-resistant IL-18 (DR-18) that displayed the low affinity to IL-18 binding protein while maintaining the signaling cascade when binding to its receptor (T. Zhou et al., 2020). These all emphasized the role of this cytokine in cancer immunotherapy.

In this work, we tried to improve the aggregation phenomenon of our modified IL-18 found at the high concentration (data not shown). Although the improvement of efficiency of our IL-18 could enhance the satisfactory result from the study, the aggregation has still been the problem because of the unpredictable activity and immunogenicity results. This was revealed by several types of FDA-approved alpha-helical cytokines, such as IL-2 (Fatima et al., 2012), IFN-β-1b (Lipiäinen et al., 2015) or granulocyte colony stimulating factor (G-CMS) (Krishnan et al., 2002) that were found to form multimer precipitation in some condition, especially physiological condition. The aggregation may result in loss of activity or induction of unfavorable immune response. For IL-18, Yamamoto and colleagues reported that the free surface cysteines, including C38, C68, C76 and C127 may contribute to IL-18 aggregation based on the computational structure prediction (Yamamoto et al., 2004). After the replacement of these cysteine by serine and the exposure of oxidative stress, the C-to-S mutations tend to form aggregation lower than wild-type IL-18, especially when all four surface cysteines were replaced (Yamamoto et al., 2004). This is in accordance with our study that when applied all these modifications to IL-18 DM, the fluorescent signal corresponding to protein aggregation was lower compared to IL-18 DM and wild-type. This suggested the contribution of surface cysteine on intermolecular bonding which also found in other cytokines (Karpusas et al., 1997; Lipiäinen et al., 2015). For example, the cysteine to serine substitution was performed for IFN-β-1b, which has been commercially used to treat relapsing forms of multiple sclerosis (MS) to increase the stability of this cytokine (Lin, 1998). The aggregation due to cysteine residue was also found in IL-31 which the formation of disulfide bond occurs at the intracellular levels (Shen et al., 2011). The replacement of these cysteine residues by serine also helped to improve the aggregation phenomenon (Shen et al., 2011). Interestingly, human α-synuclein is another case that emphasized the role of cysteine in protein stability. The aggregation of α-synuclein in Lewy bodies in midbrain dopamine neurons is usually associated with Parkinson's disease. Importantly, amino acid replacement of tyrosine by cysteine showed the increasing aggregation rate under the oxidative stress led to the cellular toxicity which may be associated with Parkinson's disease (W. Zhou & Freed, 2004).

In addition to the decrease of aggregation rate under oxidative condition, IL-18 DM1234 showed the higher ability to induce IFN-γ from NK-92MI cell compared to IL-18 DM. This may be caused by the structural changes of IL-18 DM1234 that led to the more suitable form for receptor binding. As our MD simulation revealed, D35 of IL-18 DM1234 changed its direction closer to V125 and S127 of IL-18 receptor compared to IL-18 WT and IL-18 DM. This probably led to the formation of stronger hydrogen bonds between these molecules. Importantly, this interaction was reported to played an important role for stabilizing α-helix structure of IL-18 that mediated the interaction between IL-18 and IL-18 receptor α (Tsutsumi et al., 2014). One another explanation is that the replacement of cysteine by serine may increase the surface polarity since serine showed that less hydrophilic index compared to cysteine (Kyte & Doolittle, 1982) and this scenario may improve IL-18-receptor binding. The reduction of aggregation rate might be another factor that improve the efficacy of this cytokine since it may increase the active form of IL-18 DM1234 in the system.

5. Conclusion

In summary, we have successful produced IL-18 mutation variants from *E. coli* expression system. Although the most of protein was expressed as inclusion body, we accomplished the refolding method yielding the soluble form of IL-18 with activity. From all of results we presented, the mutation of surface cysteine to serine of IL-18 DM could reduce the aggregation prone while enhanced the activity. Despite the deep mechanism of this scenario has not been elucidated, the possibility may be from the structural changes that led to the more appropriate form of IL-18 and receptor binding. The increase of active IL-18 resulted

from the lower aggregation rate may also help it activity. Further study regarding to the mechanism of this scenario must be useful to apply for other proteins or biologic drugs.

Acknowledgments

We are grateful to the Central Research Laboratory, Faculty of Medicine, Prince of Songkla University for the use of all laboratory facilities. We also would like to thank Mr. David Patterson of the International Affairs Office, Faculty of Medicine, Prince of Songkla University for manuscript proofreading and language editing service.

Conflict of Interests

The authors declare that there no conflict of interests.

Author Contributions

Jirakrit Saetang: Conceptualization; data curation; investigation; methodology; writing – original draft; writing – review and editing; visualization; validation. **Niran Roongsawang:**Conceptualization; data curation; writing – review and editing.**Surasak Sangkhathat:** Conceptualization; validation.**Supayang Piyawan Voravuthikunchai:** Funding acquisition.**Natnaree Sangkaew:** Investigation. **Napat Prompat:**Investigation. **Teerapol Srichana:** Funding acquisition.**Varomyalin Tipmanee:** Conceptualization; data curation; investigation; methodology.

References

Berendsen, H. J. C., Postma, J. P. M., Gunsteren, W. F. van, DiNola, A., & Haak, J. R. (1984). Molecular dynamics with coupling to an external bath. *The Journal of Chemical Physics* , *81* (8), 3684–3690.

Bringans, S., Eriksen, S., Kendrick, T., Gopalakrishnakone, P., Livk, A., Lock, R., & Lipscombe, R. (2008). Proteomic analysis of the venom of Heterometrus longimanus (Asian black scorpion). *Proteomics* ,*8* (5), 1081–1096.

Case, D., Aktulga, H., Belfon, K., Ben-Shalom, I., Brozell, S., Cerutti, D., Cheatham, III, T., & Cisneros, G. (2021). *Amber 2021* . University of California, San Francisco.

Castro, F., Cardoso, A. P., Gonçalves, R. M., Serre, K., & Oliveira, M. J. (2018). Interferon-Gamma at the Crossroads of Tumor Immune Surveillance or Evasion. *Frontiers in Immunology* , *9* , 847.

Fabbi, M., Carbotti, G., & Ferrini, S. (2015). Context-dependent role of IL-18 in cancer biology and counter-regulation by IL-18BP.*Journal of Leukocyte Biology* , *97* (4), 665–675.

Fatima, U., Singh, B., Subramanian, K., & Guptasarma, P. (2012). Insufficient (Sub-native) Helix Content in Soluble/Solid Aggregates of Recombinant and Engineered Forms of IL-2 Throws Light on How Aggregated IL-2 is Biologically Active. *The Protein Journal* , *31* (7), 529–543.

Humphrey, W., Dalke, A., & Schulten, K. (1996). VMD: Visual molecular dynamics. *Journal of Molecular Graphics* , *14* (1), 33–38, 27–28.

Karpusas, M., Nolte, M., Benton, C. B., Meier, W., Lipscomb, W. N., & Goelz, S. (1997). The crystal structure of human interferon beta at 2.2-A resolution. *Proceedings of the National Academy of Sciences of the United States of America* , *94* (22), 11813–11818.

Kato, Z., Jee, J., Shikano, H., Mishima, M., Ohki, I., Ohnishi, H., Li, A., Hashimoto, K., Matsukuma, E., Omoya, K., Yamamoto, Y., Yoneda, T., Hara, T., Kondo, N., & Shirakawa, M. (2003). The structure and binding mode of interleukin-18. *Nature Structural Biology* , *10* (11), 966–971.

Kim, S. H., Azam, T., Yoon, D. Y., Reznikov, L. L., Novick, D., Rubinstein, M., & Dinarello, C. A. (2001). Site-specific mutations in the mature form of human IL-18 with enhanced biological activity and decreased neutralization by IL-18 binding protein. *Proceedings of the National Academy of Sciences of the United States of America* ,*98* (6), 3304–3309.

Kim, S.-H., Azam, T., Novick, D., Yoon, D.-Y., Reznikov, L. L., Bufler, P., Rubinstein, M., & Dinarello, C. A. (2002). Identification of amino acid residues critical for biological activity in human interleukin-18. *The Journal of Biological Chemistry* , *277* (13), 10998–11003.

Krishnan, S., Chi, E. Y., Webb, J. N., Chang, B. S., Shan, D., Goldenberg, M., Manning, M. C., Randolph, T. W., & Carpenter, J. F. (2002). Aggregation of granulocyte colony stimulating factor under physiological conditions: Characterization and thermodynamic inhibition. *Biochemistry* , *41* (20), 6422–6431.

Kyte, J., & Doolittle, R. F. (1982). A simple method for displaying the hydropathic character of a protein. *Journal of Molecular Biology* ,*157* (1), 105–132.

Li, A., Kato, Z., Ohnishi, H., Hashimoto, K., Matsukuma, E., Omoya, K., Yamamoto, Y., & Kondo, N. (2003). Optimized gene synthesis and high expression of human interleukin-18. *Protein Expression and Purification* , *32* (1), 110–118.

Lin, L. (1998). Betaseron. *Developments in Biological Standardization* , *96* , 97–104.

Lipiäinen, T., Peltoniemi, M., Sarkhel, S., Yrjönen, T., Vuorela, H., Urtti, A., & Juppo, A. (2015). Formulation and Stability of Cytokine Therapeutics. *Journal of Pharmaceutical Sciences* , *104* (2), 307–326.

Mailliard, R. B., Alber, S. M., Shen, H., Watkins, S. C., Kirkwood, J. M., Herberman, R. B., & Kalinski, P. (2005). IL-18–induced CD83+CCR7+ NK helper cells. *The Journal of Experimental Medicine* ,*202* (7), 941–953.

Nakamura, K., Kassem, S., Cleynen, A., Chrétien, M.-L., Guillerey, C., Putz, E. M., Bald, T., Förster, I., Vuckovic, S., Hill, G. R., Masters, S. L., Chesi, M., Bergsagel, P. L., Avet-Loiseau, H., Martinet, L., & Smyth, M. J. (2018). Dysregulated IL-18 Is a Key Driver of Immunosuppression and a Possible Therapeutic Target in the Multiple Myeloma Microenvironment. *Cancer Cell* , *33* (4), 634-648.e5.

Okamura, H., Nagata, K., Komatsu, T., Tanimoto, T., Nukata, Y., Tanabe, F., Akita, K., Torigoe, K., Okura, T., & Fukuda, S. (1995). A novel costimulatory factor for gamma interferon induction found in the livers of mice causes endotoxic shock. *Infection and Immunity* ,*63* (10), 3966–3972.

Robertson, M. J., Kirkwood, J. M., Logan, T. F., Koch, K. M., Kathman, S., Kirby, L. C., Bell, W. N., Thurmond, L. M., Weisenbach, J., & Dar, M. M. (2008). A dose-escalation study of recombinant human interleukin-18 using two different schedules of administration in patients with cancer. *Clinical Cancer Research: An Official Journal of the American Association for Cancer Research* , *14* (11), 3462–3469.

Robertson, M. J., Mier, J. W., Logan, T., Atkins, M., Koon, H., Koch, K. M., Kathman, S., Pandite, L. N., Oei, C., Kirby, L. C., Jewell, R. C., Bell, W. N., Thurmond, L. M., Weisenbach, J., Roberts, S., & Dar, M. M. (2006). Clinical and biological effects of recombinant human interleukin-18 administered by intravenous infusion to patients with advanced cancer. *Clinical Cancer Research: An Official Journal of the American Association for Cancer Research* , *12* (14 Pt 1), 4265–4273.

Saetang, J., Chonpathompikunlert, P., Sretrirutchai, S., Roongsawang, N., Kayasut, K., Voravuthikunchai, S. P., Sukketsiri, W., Tipmanee, V., & Sangkhathat, S. (2020). Anti-cancer effect of engineered recombinant interleukin 18. *Advances in Clinical and Experimental Medicine: Official Organ Wroclaw Medical University* , *29* (10), 1135–1143.

Saetang, J., Puseenam, A., Roongsawang, N., Voravuthikunchai, S. P., Sangkhathat, S., & Tipmanee, V. (2016). Immunologic Function and Molecular Insight of Recombinant Interleukin-18. *PloS One* ,*11* (8), e0160321.

Schymkowitz, J., Borg, J., Stricher, F., Nys, R., Rousseau, F., & Serrano, L. (2005). The FoldX web server: An online force field. *Nucleic Acids Research* , *33* (suppl_2), W382–W388.

Shen, M., Siu, S., Byrd, S., Edelmann, K. H., Patel, N., Ketchem, R. R., Mehlin, C., Arnett, H. A., & Hasegawa, H. (2011). Diverse functions of reactive cysteines facilitate unique biosynthetic processes of aggregate-

prone interleukin-31. *Experimental Cell Research* ,*317* (7), 976–993.

Srivastava, S., Salim, N., & Robertson, M. J. (2010). Interleukin-18: Biology and role in the immunotherapy of cancer. *Current Medicinal Chemistry* , *17* (29), 3353–3357.

Swencki-Underwood, B., Cunningham, M. R., Heavner, G. A., Blasie, C., McCarthy, S. G., Dougherty, T., Brigham-Burke, M., Gunn, G. R., Goletz, T. J., & Snyder, L. A. (2006). Engineering human IL-18 with increased bioactivity and bioavailability. *Cytokine* , *34* (1–2), 114–124.

Tsutsumi, N., Kimura, T., Arita, K., Ariyoshi, M., Ohnishi, H., Yamamoto, T., Zuo, X., Maenaka, K., Park, E. Y., Kondo, N., Shirakawa, M., Tochio, H., & Kato, Z. (2014). The structural basis for receptor recognition of human interleukin-18. *Nature Communications* ,*5* , 5340.

Yamamoto, Y., Kato, Z., Matsukuma, E., Li, A., Omoya, K., Hashimoto, K., Ohnishi, H., & Kondo, N. (2004). Generation of highly stable IL-18 based on a ligand-receptor complex structure. *Biochemical and Biophysical Research Communications* , *317* (1), 181–186.

Zhou, T., Damsky, W., Weizman, O.-E., McGeary, M. K., Hartmann, K. P., Rosen, C. E., Fischer, S., Jackson, R., Flavell, R. A., Wang, J., Sanmamed, M. F., Bosenberg, M. W., & Ring, A. M. (2020). IL-18BP is a secreted immune checkpoint and barrier to IL-18 immunotherapy.*Nature* , *583* (7817), 609–614.

Zhou, W., & Freed, C. R. (2004). Tyrosine-to-Cysteine Modification of Human α-Synuclein Enhances Protein Aggregation and Cellular Toxicity *.*Journal of Biological Chemistry* , *279* (11), 10128–10135.

Figure legends

Figure 1. The crystal structure of IL-18 WT and receptor. (A) The ribbon structure of mature human IL-18 (3WO3) retrieved from Protein Data Bank. Surface cysteines substituted in this study were indicated. (B) The ribbon structure of IL-18 (cyan) with IL-18 receptor α (yellow).

Figure 2. SDS-PAGE analysis of recombinant IL-18 before and after refolding. (A) SDS-PAGE analysis of soluble protein and insoluble protein obtained after IL-18 expression by *E. coli* . Lane: M = protein marker, 1 = soluble protein from IL-18 WT expressing *E. coli* , 2 = soluble protein from IL-18 DM expressing *E. coli* , 3 = soluble protein from IL-18 DM1234 expressing *E. coli* , 4 = insoluble protein from IL-18 WT expressing *E. coli* , 5 = insoluble protein from IL-18 DM expressing *E. coli* , 6 = insoluble protein from IL-18 DM1234 expressing *E. coli* . (B) SDS-PAGE analysis of recombinant IL-18 after protein refolding. M = protein marker, 1 = IL-18 WT, 2 = IL-18 DM, 3 = IL-18 DM1234. All samples were loaded onto 12% SDS-PAGE.

Figure 3. LC-MS/MS analysis of recombinant mature IL-18. (A) Tryptic peptide map of recombinant mature IL-18 produced by *E. coli* expression system. The identified peptides are shown in red, (B) Identified tryptic peptide fragment derived from IL-18.

Φιγυρε 4. Αγγρεγατιον ανδ ΙΦΝ-γ ινδυστιον ασσαψς οφ εαση τψπε οφ ΙΛ-18. (A) The signal obtained from ProteoStat protein aggregation assay of each type of refolded IL-18 was shown. (B) IFN-γ induction assay with each type of IL-18. NK-92MI cells were treated with various concentrations of IL-18 for 16-18 hours. IFN-γ was measured in the supernatant by ELISA. All figures illustrated results represent the mean ± SD of three independent experiments. *$p < 0.05$.

Figure 5. Structural analysis revealed by MD simulation. (A) Structural alignment of three types of IL-18. The binding site I is indicated in the figure. (B) The obvious different part of IL-18 DM1234 structure. The interface between binding site I of each type of IL-18 and IL-18 receptor α was demonstrated. (C) The molecular structure revealed the interaction between D35 of IL-18 WT and IL-18 DM1234 and V125 and S127 of IL-18 receptor α. The distance between interacted amino acids was indicated as angstrom (A@). (D) The interaction of D35 of IL-18 DM and V125 and S127 of IL-18 receptor α was demonstrated with the distance as angstrom (A@).

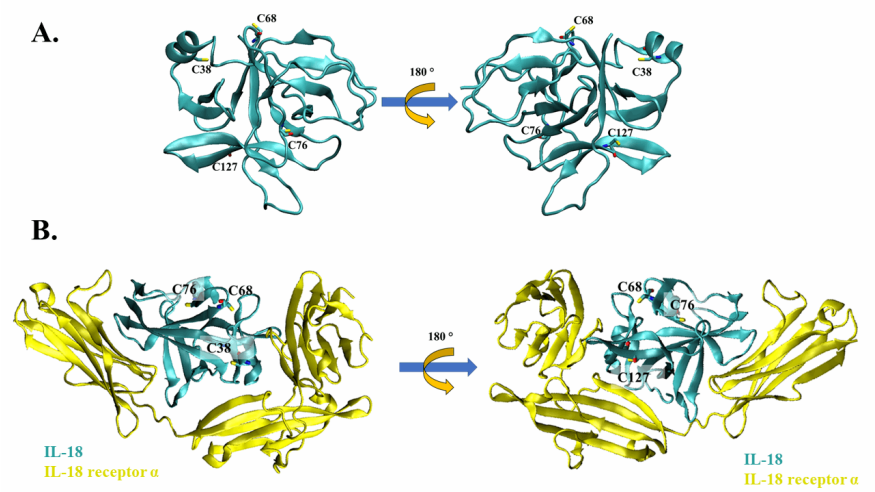

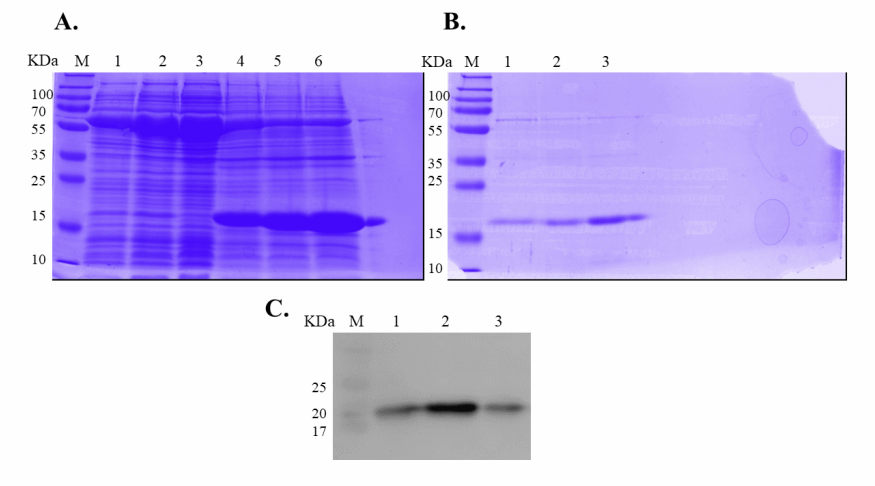

A.

```
        10         20         30         40
YFGKLKSKLS VIRNLNDQVL FIDQGNRPLF EDMTDSDCRD
        50         60         70         80
NAPRTIFIIS MYKDSQPRGM AVAISVKCEK ISTLSCENKI
        90        100        110        120
ISFKEMNPPD NIKDTKSDII FFQRSVPGHD NKMQFESSSY
       130        140        150        157
EGYFLACEKE RDLFKLILKK EDELGDRSIM FTVQNED
```

B.

m/z	Molecular weight (MW)	Position	Peptide
1024.4285	3070.2637	14-39	NLNDQVLFIDQGNRPLFEDMTDSDCR
566.9090	1697.7052	45-58	TIFIISMYKDSQPR
453.1910	904.3675	59-67	GMAVTISVK
549.2268	1644.6586	80-93	IISFKEMNPPDNIK
467.8337	1400.4791	86-96	EMNPPDNIKDTK
457.1798	1368.5174	94-104	DTKSDIIFFQR
513.2092	1024.4038	97-104	SDIIFFQR
481.1692	960.3239	140-147	KEDELGDR
592.1975	1182.3805	148-157	SIMFTVQNED